Physics and Chemistry of Minerals (2019) 46:743–749
https://doi.org/10.1007/s00269-019-01035-z

ORIGINAL PAPER

Destruction of fayalite and formation of iron and iron hydride at high hydrogen pressures

Vadim S. Efimchenko[1] · Nicolay V. Barkovskii[1] · Vladimir K. Fedotov[1] · Konstantin P. Meletov[1] · Vladimir M. Chernyak[1] · Kirill I. Khryapin[2]

Received: 11 January 2019 / Accepted: 23 April 2019 / Published online: 2 May 2019

Abstract

Thermal stability of fayalite (Fe_2SiO_4) is studied at hydrogen pressures up to 7.5 GPa and temperatures up to 400 °C. Powder samples of Fe_2SiO_4 were exposed to a hydrogen or deuterium atmosphere for 24 h in the Toroid-type apparatus at pre-selected pressures and temperatures followed by quenching to the temperature of liquid nitrogen. The phase and chemical compositions of the quenched samples were examined by energy-dispersive X-ray spectroscopy, X-ray diffraction and Raman spectroscopy at ambient pressure. The chemical composition of volatile products was studied by quadrupole mass spectroscopy in the course of heating from − 196 to 20 °C in a pre-evacuated quartz tube. In these experiments, deuterated samples were used to be sure that the detected compounds could only be formed in the reaction of fayalite with the high-pressure D_2 gas. The obtained data allowed us to construct the line of thermal stability of fayalite at hydrogen pressures up to 7.5 GPa. The decomposition temperature of fayalite was proved to nonlinearly decrease from ~ 375 °C at the pressures $P_{H2} = 1.4$–2.8 GPa to ~ 175 °C at $P_{H2} = 7.5$ GPa. At higher temperatures, fayalite fully decomposed to a mixture of silica, water and metallic Fe or FeH depending on the pressure and temperatures of the hydrogenation.

Keywords Fayalite · Hydrogen · High pressure · Decomposition reaction · Silica · Iron hydride

Introduction

Olivine is known to be the most abundant mineral in the Earth upper mantle. The Earth's crust and upper mantle also contain many light elements that form various fluids: H_2O, CO_2, CH_4, H_2, etc. At pressures up to 2.5 GPa, water and hydrogen are shown to coexist as separate, immiscible phases (Bali et al. 2013). At pressures above 5 GPa (corresponding to the depths of more than 200 km), the C–O–H fluids should be in a reduced state and mainly consist of H_2 and CH_4 according to the available experimental (Sokol et al. 2009) and theoretical (Frost and McCammon 2008; Woodland and Koch 2003) data. At pressures above 6.3 GPa, the C–O–H fluids are composed of 79 mol% H_2 and 21 mol% CH_4 (Sokol et al. 2009). This composition is most likely the result of chemical reactions, such as the methane polymerization (Kolesnikov et al. 2009).

Consequently, our understanding of the processes occurring in this part of the Earth interior will be incomplete in the absence of physical and chemical data concerning the interaction of silicates with hydrogen at high pressures. In addition, this interaction is important for understanding the chemical and physical processes that occur during the birth and evolution of planetary systems, since olivine (de Vries et al. 2012) and hydrogen (Eisner 2007) are constituents of the pre-solar nebulae.

Earlier, X-ray diffraction and Raman spectroscopy revealed the penetration of hydrogen molecules into the crystal structure of forsterite (Mg_2SiO_4) at pressures up to 10 GPa and $T \sim 1000$ K (Shinozaki et al. 2012) followed by partial decomposition of forsterite to MgO and SiO_2 at higher temperatures (Shinozaki et al. 2013). Another end-member olivine compound, fayalite (Fe_2SiO_4), was earlier

Electronic supplementary material The online version of this article (https://doi.org/10.1007/s00269-019-01035-z) contains supplementary material, which is available to authorized users.

✉ Vadim S. Efimchenko
efimchen@issp.ac.ru

[1] Institute of Solid State Physics Russian Academy of Sciences, Chernogolovka, 2 Academician Ossipyan str., Moscow 142432, Russia

[2] Lomonosov Moscow State University, GSP-1, Leninskie Gory, Moscow 119991, Russia

studied only at hydrogen pressures up to 1 atm. At hydrogen pressures below 1 atm, fayalite Fe_2SiO_4 is known to decompose to quartz, iron and water after heating above 800 °C (Massieon et al. 1993).

The present paper reports on the thermal destruction of fayalite at hydrogen pressures up to 7.5 GPa. Each sample was hydrogenated by exposing to a hydrogen pressure from 1.4 to 7.5 GPa and a temperature up to 400 °C. After the hydrogenation was complete, the sample was rapidly cooled to the boiling temperature of N_2. The quenched samples were studied by X-ray diffraction, Raman spectroscopy, energy-dispersive X-ray spectroscopy (EDX) at ambient pressure and $T = -188$ °C and 25 °C. The composition of the volatile substances in the quenched samples was examined by quadrupole mass spectroscopy in the regime of heating the deuterated quenched samples from − 196 to 20 °C.

Experimental methods

The initial samples of fayalite powder were synthesized by solid-state reaction of silica, carbonyl iron and hematite at $T = 1000$ °C in a reduced atmosphere. The as-prepared sample contained a certain amount of particles of unreacted iron, which were further removed by a permanent magnet.

Hydrogenation of fayalite was carried out in a Toroid-type high-pressure apparatus with a squirrel-type heater made of Nichrome wire 0.5 mm in diameter and aminoborane (NH_3BH_3) used as an internal hydrogen source (Antonov et al. 2017). The fayalite sample and aminoborane were placed together in a high-pressure cell made of Teflon or copper and separated from each other by a Pd foil as shown in Fig. 1. To evolve hydrogen, aminoborane was decomposed at $P = 1.5$ GPa by heating to $T = 280$°C. Aminoborane is known to decompose in several stages, which include the formation of volatile compounds such as NH_2BH_2 and NHBH; however, all intermediate compounds are thermally unstable at $T > 200$ C and transform to a binary mixture of gaseous H_2 and solid BN (Storozhenko et al. 2005, Nylén et al. 2009). The temperature and pressure of the H_2 gas, thus, produced were than varied along the routes indicated in Fig. 2 until reaching the pre-selected $T = 25$–400°C and $P = 1.4$–7.5 GPa. The temperature was measured with an accuracy of ± 10°C with a Chromel–Alumel thermocouple. The pressure was estimated with an accuracy of ± 0.3 GPa using the pressure/ram load dependence determined in separate experiments. The amount of hydrogen in the reaction cell always exceeded the amount of hydrogen absorbed by the sample by 2–3 times.

The powder sample of Fe_2SiO_4 was exposed to the preselected conditions for 24 h. Then, the high-pressure apparatus with the sample inside it was quenched to the liquid N_2 temperature and the pressure was released. The high-pressure apparatus was disassembled under liquid nitrogen and the sample was retrieved from the cell and stored in liquid N_2 until the measurements.

The elemental composition of the samples was obtained at room temperature by energy-dispersive X-ray spectroscopy using Supra 50VP scanning electron microscope with a field emission gun and an Oxford Inca Energy 450 energy-dispersive X-ray analysis system.

The composition of the volatile products of the fayalite hydrogenations was determined on the deuterated samples using a quadrupole mass spectroscope XT100M Extorr with the electron beam ionization. The energy of electrons in the beam was 70 eV.

Raman spectra from the hydrogenated and initial samples were recorded in a back-scattering geometry using a

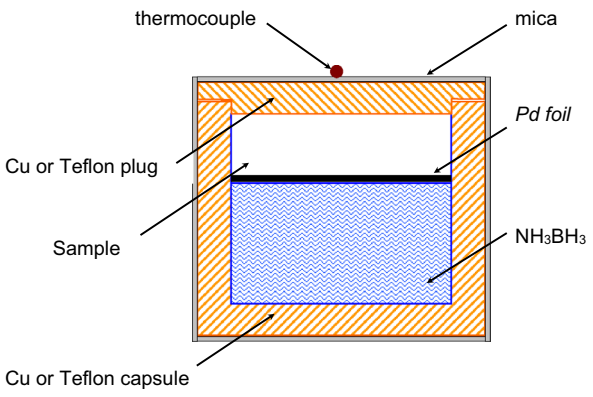

Fig. 1 Schematic diagram of a high-pressure cell with aminoborane NH_3BH_3 used as a solid hydrogen source. The external diameter of the cell is 8.5 mm, the thickness of its walls is 0.7 mm

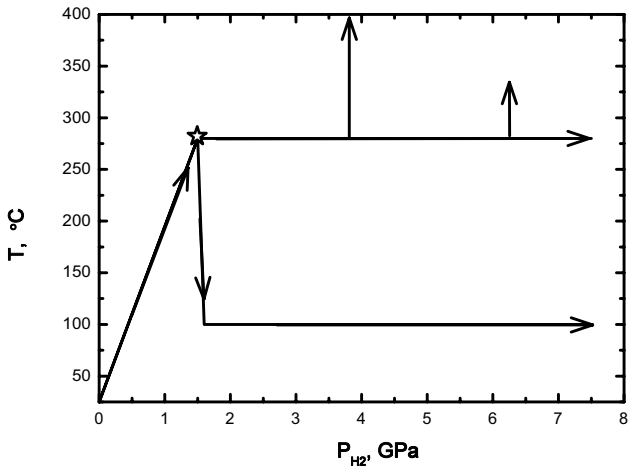

Fig. 2 The temperature and pressure routes of the fayalite hydrogenation. The arrows indicate the ways of changing the pressure and temperature. The asterisk shows the conditions of decomposition of the NH_3BH_3 or AlD_3 compound used to fill the high-pressure cell with a H_2 or D_2 gas, respectively

micro-Raman setup comprised of an Acton SpectraPro-2500i spectrograph and a CCD Pixis2K detector system cooled down to − 70 °C. The measurements were performed near the liquid nitrogen temperature in the spectral range from 140 to 4500 cm^{-1}. The 532 nm line of a single-mode YAG CW diode pumped laser was focused on the sample by an Olympus 50 × objective in a ~ 2-μm diameter spot that was slightly defocused due to the light refraction in the nitrogen vapors. The spatial resolution was also ~ 2 μm and the spectral resolution varied between 2.3 and 4.1 cm^{-1}. The laser line in the scattered beam was suppressed by a super-notch filter with the optical density OD = 6 and bandwidth ~ 160 cm^{-1}, while the beam intensity before the sample was ~ 5 mW. The data acquisition time was 120 s.

The quenched samples were also studied by powder X-ray diffraction at ambient pressure and − 188 °C using a Siemens D500 diffractometer equipped with a home-designed nitrogen cryostat that permitted loading metastable powder samples without their intermediate warming.

Results

According to the results of energy-dispersive X-ray spectroscopy (EDX) presented in Table 1, the concentrations of iron, silicon and oxygen in the initial sample were close to those of the fayalite compound Fe_2SiO_4 with a small excess of iron. The small amount of carbon resulted from the luminescence of the sample substrate. An X-ray examination of these samples at room temperature showed them to be single-phase fayalite with an orthorhombic Pnma structure and lattice parameters $a = 10.471(6)$ Å, $b = 6.087(4)$ Å, $c = 4.817(4)$ Å in agreement with (Anthony et al. 2001).

The quenched samples of hydrogenated fayalite were studied by scanning electron microscopy (SEM), energy-dispersive X-ray spectroscopy (EDX), X-ray diffraction, Raman spectroscopy and Quadrupole mass spectroscopy. Figure 1S (Online Resource 1) presents a SEM image of the initial sample. Figures 2S and 3S (Online Resource 1) show two different areas on the surface of the sample hydrogenated at $P = 7.5$ GPa and $T = 280$ °C. As one can see, the surface of the hydrogenated sample is covered with white and gray particles. This heterogeneity of the sample surface implies the destruction of the fayalite compound.

Table 2a presents the mean contents of the elements on the surface of the hydrogenated sample inside the 200×150 μm square shown on Fig. 2S (Online Resource 1). As it is seen, the obtained atomic ratio Fe/Si = 1.44 is significantly less than the approximately stoichiometric ratio of the initial sample.

The white particles bounded with the rectangle on Fig. 3S (Online Resource 1) consist of silicon dioxide SiO_2 with a small admixture of iron. The presence of the particles of nearly pure SiO_2 in the hydrogenated samples additionally confirms the decomposition of the hydrogenated faylite.

The decomposition of the hydrogenated fayalite and the formation of silicon dioxide were also confirmed by Raman spectroscopy for the samples hydrogenated at $P = 3.3$ and 7.5 GPa. Figure 3 shows the Raman spectra collected at ambient pressure on the quenched samples submerged in liquid nitrogen. As seen from Fig. 3, the lines of fayalite disappeared after the increase in the hydrogenation temperature from 200 to 220 °C at $P = 3.3$ GPa and from 150 to 200 °C at $P = 7.5$ GPa. Instead of the fayalite lines, a few peaks of the coesite phase of SiO_2 arose in the Raman spectra. At the same time, there were no lines of any iron-containing compounds. This could be due to the formation of a metallic iron-containing phase invisible in the Raman spectra.

To verify the formation of such a phase, we hydrogenated a few samples at $P = 1.4$–7.5 GPa and $T = 25$–$400°$ C and studied them by X-ray diffraction at ambient pressure and

Table 1 The composition of the initial sample determined by energy-dispersive X-ray spectroscopy

Element	Weight%	Atomic%	Atomic ratio element/Si
C	1.24	2.86	0.2 (2)
O	34.29	59.30	5 (2)
Si	12.05	11.87	1
Fe	52.42	25.97	2.2 (1)
Totals	100	100	

The expected experimental errors are indicated in the rightmost column

Table 2 The total composition of the sample hydrogenated at $P = 7.5$ GPa and $T = 280$ °C and examined by EDX

Element	Weight%	Atomic%	Atomic ratio element/Si
(a)			
C K	1.80	4.48	0.22
O K	24.37	45.57	2.26
Mg K	0.53	0.65	0.03
Si K	18.94	20.18	1
Fe K	54.36	29.12	1.44
Total	100.00		
(b)			
O K	54.62	68.27	2.19
Si K	43.76	31.16	1
Fe K	1.61	0.58	0.019
Total	100.00		

The data in (a) and (b) are averaged over the areas marked with the rectangles on Figs. 2S and 3S (Online Resource 1), respectively

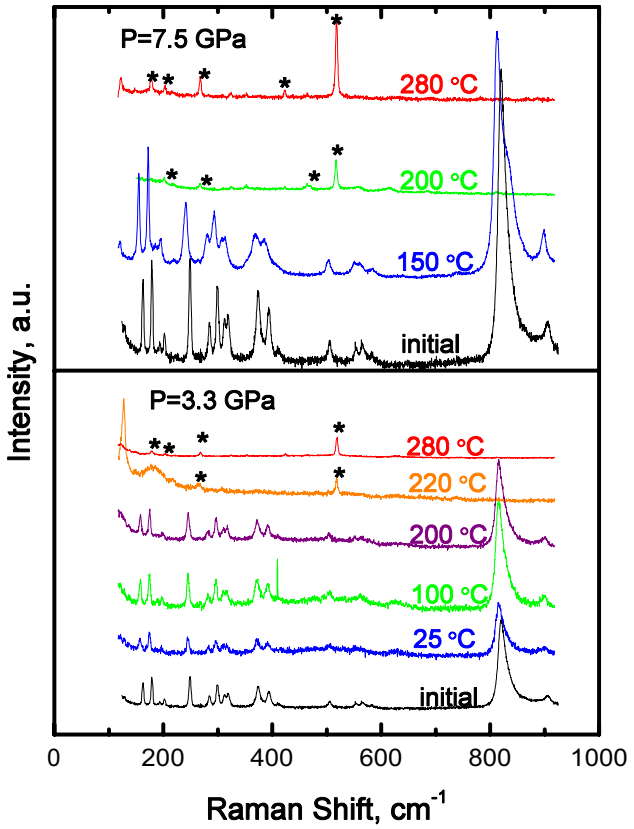

Fig. 3 Raman spectrum of the fayalite (Fe_2SiO_4) sample in the initial state and after hydrogenation at $P = 7.5$ GPa (upper figure) and 3.3 GPa (lower figure) measured at liquid nitrogen temperature and ambient pressure. The labels denote the temperature of the hydrogenation. Asterisks mark the peaks corresponding to the coesite phase of SiO_2

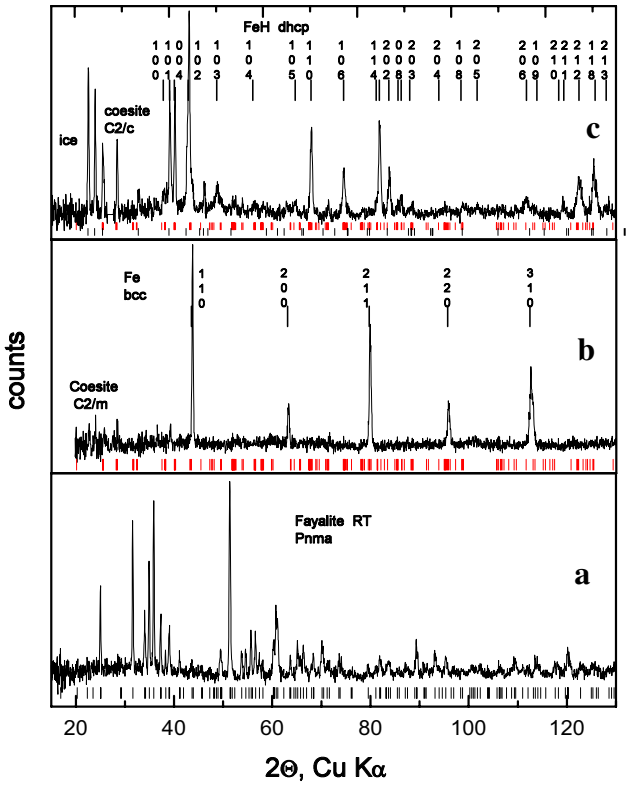

Fig. 4 X-ray diffraction patterns of the samples hydrogenated at $T = 280$ °C and pressures of 2.8 (a), 3.3 (b) and 7.5 (c) GPa. All spectra were collected on the quenched samples at ambient pressure and $T = -180$ °C using CuKα radiation

$T = -180$ °C. Typical X-ray diffraction patterns are shown on Fig. 4. Phase compositions of the hydrogenated samples determined by profile analysis of the obtained X-ray patterns are listed in Table 3. As one can see, the initial *Pnma* fayalite structure collapsed after the hydrogenation at $T = 400$ °C and $P = 1.4$–2.8 GPa and at a much lower temperatures of $T = 200$–280 °C at higher pressures of $P = 3.3$–7.5 GPa.

Depending on the hydrogenation pressure, these decomposed samples consisted of two phases: a silicon dioxide phase in the form of quartz or coesite and a metallic phase of bcc iron or dhcp iron hydide (bcc = body-centered cubic; dhcp = double-hexagonal close-packed). As seen from Table 3, phase compositions of these samples correspond to the atomic ratio Fe/Si < 2 in agreement with the EDX results (Table 2a). The deficiency in iron compared to the initial composition of the fayalite sample (Table 1) is likely to be due to the partial dissolution of iron in the Pd foil used to separate the sample and NH_3BH_3 in the high-pressure cell. Some iron could also be lost when disassembling the high-pressure cell, because the magnetic Fe and FeH particles could stick to the steel tools.

The chemical composition of volatile products resulted from the hydrogen-induced decomposition of fayalite was studied by quadrupole mass spectroscopy by heating the quenched samples from − 196 to 20 °C in a pre-evacuated quartz tube. In these experiments, we used deuterated samples to be sure that the detected substances could only be formed in the reaction of fayalite with the D_2 gas. As shown on Fig. 5, heating the deuterated sample to − 35 °C led to the appearance of strong peaks at $m/e = 3$ and 4, thus signaling on the decomposition of the iron deuteride. Further heating led to the appearance of lines at 19 and 20 *m/e*, which could be attributed to DHO and D_2O molecules. There were no lines attributable to SiD_x at any studied temperatures.

In all our experiments, the amount of NH_3BH_3 placed in the high-pressure cell was chosen so as to release molecular hydrogen in an amount corresponding to the molar ratio $H_2/Fe_2SiO_4 = 5$. This warranted that molecular hydrogen was always in access in the high-pressure cell. Depending on whether or not the dhcp iron hydride was formed, two paths of the reaction of fayalite with high-pressure hydrogen were, therefore, possible. At hydrogen pressures up to 3.3 GPa, fayalite decomposed by the reaction:

$$Fe_2SiO_4 + 2H_2 \rightarrow 2Fe(bcc) + SiO_2 + 2H_2O. \quad (1)$$

Table 3 Pressures and temperatures of hydrogenation of fayalite and phase compositions of the resulting hydrogenated samples according to X-ray diffraction

P (GPa)	*T* (°C)	Fayalite (mol%)	Fe bcc (mol%)	FeH (dhcp) (mol%)	SiO_2 (mol%)
1.4	350	100	0	0	0
	400	0	44	0	56 (quartz)
2.5	280	100	0	0	0
	350	100	0	0	0
	400	0	41.4	0	58.6 (quartz)
2.8	280	100	0	0	0
	400	0	42.3	0	57.7 (quartz)
3.3	25	100	0	0	0
	100	100	0	0	0
	200	99.8	0.2	0	0
	220	0	36.6	0	83.4 (coesite)
	280	0	55	0	45 (coesite)
7.5	150	100	0	0	0
	200	25	15	60	0
	280	0	0	61.2	38.8 (coesite)

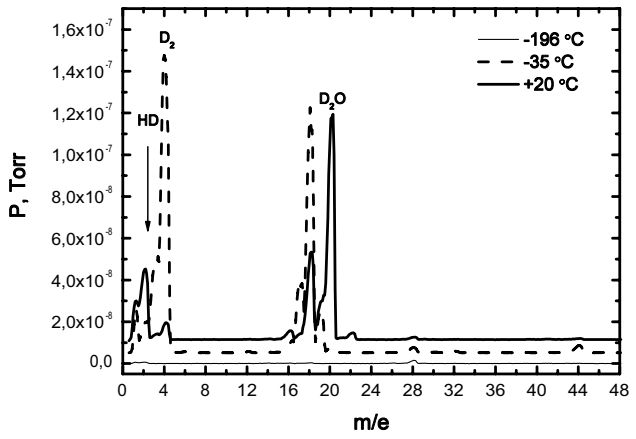

Fig. 5 Quadrupole mass spectra measured in the regime of heating the quenched samples from − 196 to + 20 °C in a pre-evacuated quartz tube. The samples were deuterated at $P = 7.5$ GPa and $T = 280$ °C

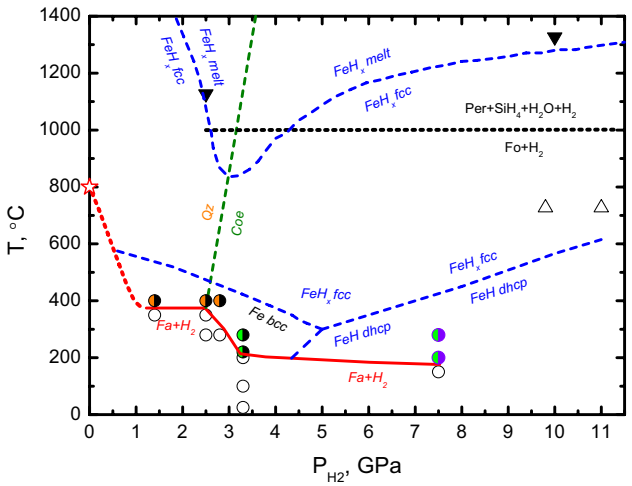

Fig. 6 The empty circles show that fayalite remained thermally stable under the indicated *T* and *P*. The orange–black and green–black circles show that fayalite decomposed, respectively, to the $Qz + FeH_x(bcc) + H_2O + H_2$ or $Coe + FeH_x(bcc) + H_2O + H_2$ mixtures. The green–violet circles indicate the decomposition of fayalite to the $Coe + FeH(dhcp) + H_2O + H_2$ mixture. The asterisk shows the decomposition temperature of fayalite determined earlier (Massieon et al. 1993). The upper boundary of the stability region of fayalite is shown by the solid red line and extended by a dotted curve into the yet unexplored pressure interval below 1.4 GPa. The empty and filled triangles indicate, respectively, that forsterite remained thermally stable (Shinozaki et al. 2012) or decomposed (Shinozaki et al. 2013). The black dotted line represents the speculative temperature of the forsterite decomposition under hydrogen pressure. The green dash and blue dash lines are the lines of phase transitions in SiO_2 (Cohen and William 1967) and in the Fe–H system (Hiroi et al. 2005)

At a pressure of 7.5 GPa, the dhcp iron hydride was formed instead of bcc iron:

$$Fe_2SiO_4 + 3H_2 \rightarrow 2FeH(dhcp) + SiO_2(coesite) + 2H_2O. \quad (2)$$

Discussion

In the *T*–*P* diagram of Fig. 6, the orange–black, green–black and green–violet circles stand for the samples of fayalite destructed, while exposed to the indicated pressure and temperature in an atmosphere of molecular hydrogen. The empty circles show the *P*–*T* conditions under which the fayalite retained its initial crystal structure. Using these data, we constructed an approximate line of the fayalite decomposition depicted in the figure by the red line. Other lines in the figure show phase transitions in the products of fayalite decomposition (Cohen and William 1967; Hiroi

et al. 2005). As one can see, the decomposition temperature of fayalite is 375 °C at hydrogen pressures 1.4–2.5 GPa. The decomposition temperature drops to 210 °C when the fayalite decomposition line crosses the line of the quartz–coesite phase transition (Cohen and William 1967). Further increase in the hydrogenation pressure up to 7.5 GPa gradually lowers the decomposition temperature to 175 °C.

The drop in the temperature of decomposition of fayalite from 375 to 210 °C at pressures of 2.5–3.3 GPa, as well as its further decrease to 175 °C at $P = 7.5$ GPa can be explained by phase transitions in the decomposition products of fayalite. The first drop is likely to be due to the quartz–coesite phase transformation of the silica. Since coesite is denser than quartz, this shifts equilibrium (1) to the right and lowers the temperature of the fayalite decomposition. Similarly, the decrease in the volume of the system due to the formation of iron hydride could further lead to the observed decrease in this temperature from 210 °C at 3 GPa tp 175 °C at 7.5 GPa. The maximal value $T = 375$ °C of the decomposition temperature of fayalite, observed in our experiments, is significantly lower than $T = 800$ °C, previously obtained at a hydrogen pressure below 1 atm (Massieon et al. 1993). This suggests a strong drop in the decomposition temperature of fayalite at pressures below 1.4 GPa. The possible behavior of the $T(P)$ dependence in this pressure interval is shown in Fig. 6 by the red-dotted line.

According to (Shinozaki et al. 2012), forsterite persists after hydrogenation at $P = 9.8$ and 11 GPa and $T = 723$ °C. A further increase in the temperature to 1100–1500 °C in a wide range of hydrogen pressures of 2.5–14 GPa leads to a partial decomposition of forsterite to periclase (MgO) and SiO_2 (Shinozaki et al. 2013). Based on these data, we concluded that forsterite should decompose after heating above 1000 °C at hydrogen pressures $P \geq 2.5$ GPa. This is shown in Fig. 6 by the black-dotted line. A comparison of the decomposition temperatures of fayalite and forsterite led us to the conclusion that the stability of olivine under hydrogen pressure strongly depends on the Mg/Fe ratio. Besides, the decomposition products of the iron- and magnesium-containing olivines are different. As described above, Fe^{2+} cations are always completely reduced from fayalite Fe_2SiO_4 under hydrogen pressure and form bcc iron or dhcp iron hydride. In contrast, magnesium metal is never formed as a decomposition product of forsterite Mg_2SiO_4 in a hydrogen atmosphere. Magnesium cations are always bound to oxygen anions and form periclase MgO. It can also be noted in this connection that a separate study of the MgO–H_2 system showed the persistence of periclase even after its hydrogenation at $P = 3.2$ GPa and $T = 1430$ °C (Shinozaki et al. 2013).

In a hydrogen atmosphere, silica SiO_2 completely decomposes to monosilane SiH_4 and water at temperatures above 1000 °C (Shinozaki et al. 2014; Futera et al. 2017). At pressures above 1.4 GPa and temperatures above 1000 °C, the reactions (1) and (2) of hydrogen with, respectively, forsterite and fayalite should be rewritten as:

$$Mg_2SiO_4 + 4H_2 \rightarrow 2MgO + SiH_4 + 2H_2O, \quad (3)$$

$$Fe_2SiO_4 + (6 + x)H_2 \rightarrow 2FeH_x + SiH_4 + 4H_2O, \quad (4)$$

where x is varied from 0 to 1 depending on the pressure.

It is worth noting that reaction (4) requires four additional moles of H_2 compared to the reactions (1) and (2) and therefore, it can only occur if the reaction cell contains more than 6 mol of hydrogen per 1 mol of fayalite.

The melting curve of iron hydrides under high hydrogen pressures is known to be ~ 500 °C lower than in inert medium (Hiroi et al. 2005). As a result, this curve as well as the melting curves of SiH_4 and H_2O (Katsura et al. 2010) lie below the geotherm of the Earth's mantle. Therefore, all these compounds can only exist as melts and fluids in the deeper parts of the upper mantle. Further, the denser FeH_x melt should percolate through the rocks to the center of the Earth (Ghanbarzadeh et al. 2017), while the lighter SiH_4 and H_2O fluids will rise up. Thus, the decomposition products of fayalite should completely dissolve and disappear from the hydrogenation region at pressures and temperatures corresponding to the upper part of the Earth's mantle.

Therefore, fayalite should completely disappear from the mantle or crustal rocks if it comes into contact with a large amount of hydrogen ($H_2/Fa \geq 6$). This differs from the decomposition of forsterite by reaction with the same amount of hydrogen, which enriches the rocks of the mantle with solid MgO in accordance with Eq. (3). In this regard, however, it should be mentioned that silica will not decompose unless the condition $H_2/Fa \geq 6$ is fulfilled. Also, the interaction of hydrogen and fayalite should be long enough, so that the decomposition products can leave the hydrogenation region. Otherwise, silane and water could react with each other and form mantle rocks enriched in silica.

Summary

In the present work, fayalite was hydrogenated in a Toroid-type apparatus under hydrogen pressures up to 7.5 GPa and temperatures up to 400 °C. The studies of quenched hydrogenated samples at ambient pressure by energy-dispersive X-ray spectroscopy, Raman spectroscopy, X-ray diffraction and quadrupole mass spectroscopy allowed us to construct the $T(P)$ line of the fayalite decomposition and to obtain the chemical and phase compositions of the decomposed samples. The decomposition temperature nonlinearly decreases with increasing pressure and has a plateau at $T = 375°$ C at hydrogen pressures of 1.4–2.5 GPa; then, it drops to 210 °C at the intersection with the line of the quartz–coesite phase transition and further gradually decreases to 175 °C

at $P = 7.5$ GPa. Taking into account the previous data on the decomposition of fayalite at pressures below 1 atm, we assume a decrease in its decomposition temperature from $T = 800$ to 375 °C at pressures below 1.4 GPa.

The samples hydrogenated at temperatures above their decomposition line consist entirely of a mixture of quartz (at $P < 3.3$ GPa) or coesite (at higher pressures), water and a metallic phase of iron or its hydride. Under the conditions of the Earth's mantle, these products should form FeH_x melts and SiH_4 and H_2O fluids, which migrate to the upper or lower layers of the Earth's interior, depending on their densities. Fayalite could completely disappear from the mantle rocks if it interacts with a sufficient amount of hydrogen.

Acknowledgements The research is carried out within the state task of ISSP RAS and partly supported by Grant no. 18-02-01175 from the Russian Foundation for Basic Research and by the Program "Physics of Fundamental Interactions and Nuclear Technologies" of the Russian Academy of Sciences. The authors thank Prof. Yu. A. Litvin for useful discussions.

References

Anthony JW, Bideaux RA, Bladh KW, Nichols MC (2001) Handbook of mineralogy. Mineralogical Society of America, Chantilly

Antonov VE, Bulychev BM, Fedotov VK, Kapustin DI, Kulakov VI, Sholin IA (2017) NH_3BH_3 as an internal hydrogen source for high pressure experiments. Int J Hydrog Energy 42:22454–22459. https://doi.org/10.1016/j.ijhydene.2017.03.121

Bali E, Audetat A, Keppler H (2013) Water and hydrogen are immiscible in Earth's mantle. Nature 495:220–223. https://doi.org/10.1038/nature11908

Cohen LH, William Klement Jr (1967) High-low quartz inversion: determination to 35 kilobars. J Geophys Res 72:4245–4251. https://doi.org/10.1029/JZ072i016p04245

De Vries BL, Acke B, Blommaert JADL, Waelkens C, Waters LBFM, Vandenbussche B, Olofsson G, Min M, Dominik C, Decin L, Barlow MJ, Brandeker A, Di Francesco J, Glauser AM, Greaves J, Harvey PM, Holland WS, Ivison RJ, Liseau R, Pantin EE, Pilbratt GL, Royer P, Sibthorpe B (2012) Comet-like mineralogy of olivine crystals in an extrasolar proto-Kuiper belt. Nature 490:74–76. https://doi.org/10.1038/nature11469

Eisner JA (2007) Water vapour and hydrogen in the terrestrial-planet-forming region of a protoplanetary disk. Nature 447:562–564. https://doi.org/10.1038/nature05867

Frost DJ, McCammon CA (2008) The redox state of Earth's mantle. Annu Rev Earth Planet Sci 36:389–420. https://doi.org/10.1146/annurev.earth.36.031207.124322

Futera Z, Yong X, Pan Y, Tse JS, English NJ (2017) Formation and properties of water from quartz and hydrogen at high pressure and temperature. Earth Planet Sci Lett 461:54–60. https://doi.org/10.1016/j.epsl.2016.12.031

Ghanbarzadeh S, Hesse MA, Prodanovic M (2017) Percolative core formation in planetesimals enabled by hysteresis in metal connectivity. Proc Nat Acad Sci 114:13406–13411. https://doi.org/10.1073/pnas.1707580114

Hiroi T, Fukai Y, Mori K (2005) The phase diagram and superabundant vacancy formation in Fe–H alloys revisited. J Alloy Compd 404–406:252–255. https://doi.org/10.1016/j.jallcom.2005.02.076

Katsura T, Yoneda A, Yamazaki D, Yoshino T, Ito E (2010) Adiabatic temperature profile in the mantle. Phys Earth Planet Inter 183:212–218. https://doi.org/10.1016/j.pepi.2010.07.001

Kolesnikov A, Kutcherov VG, Goncharov AF (2009) Methane-derived hydrocarbons produced under upper-mantle conditions. Nat Geosci 2:566–570. https://doi.org/10.1038/NGEO591

Massieon CC, Cutler AH, Shadman F (1993) Hydrogen reduction of iron-bearing silicates. Ind Eng Chem Res 32:1239–1244. https://doi.org/10.1021/ie00018a033

Nylén J, Sato T, Soignard E, Yarger JL, Stoyanov E, Häussermann U (2009) Thermal decomposition of ammonia borane at high pressures. J Chem Phys 131:104506–104513. https://doi.org/10.1063/1.3230973

Shinozaki A, Hirai H, Kagi H, Kondo T, Okada T, Nishio-Hamane D, Machida S, Irifune T, Kikegawa T, Yagi T (2012) Reaction of forsterite with hydrogen molecules at high pressure and temperature. Phys Chem Miner 39:123–129. https://doi.org/10.1007/s00269-011-0467-7

Shinozaki A, Hirai H, Ohfuji H, Okada T, S-i Machida, Yagi T (2013) Influence of H_2 fluid on the stability and dissolution of Mg_2SiO_4 forsterite under high pressure and high temperature. Am Min 98:1604–1609. https://doi.org/10.2138/am.2013.4434

Shinozaki A, Kagi H, Noguchi N, Hirai H, Ohfuji H, Okada T, Nakano S, Yagi T (2014) Formation of SiH_4 and H_2O by the dissolution of quartz in H_2 fluid under high pressure and temperature. Am Miner 99:1265–1269. https://doi.org/10.2138/am.2014.4798

Sokol AG, Palyanova GA, Palyanov YN, Tomilenko VN, Melensky VM (2009) Fluid regime and diamond formation in the reduced mantle: experimental constraints. Geochim Cosmochim Acta 73:5820–5834. https://doi.org/10.1016/j.gca.2009.06.010

Storozhenko PA, Svitsyn RA, Ketsko VA, Buryak AK, Ul'yanov AV (2005) Ammineborane: synthesis and physicochemical characterization. Russ J Inorg Chem 50:980–985

Woodland AB, Koch M (2003) Variation in oxygen fugacity with depth in the upper mantle beneath the Kaapvaal craton, Southern Africa. Earth Planet Sci Lett 214:295–310. https://doi.org/10.1016/S0012-821X(03)00379-0